SUPPLEMENTAL MATERIAL
Non-monotonic fluidization generated by fluctuating edge tensions in confluent tissues

Takaki Yamamoto,[1,2,*] Daniel M. Sussman,[3] Tatsuo Shibata,[1] and M. Lisa Manning[4,5,†]

[1] *Laboratory for Physical Biology, RIKEN Center for Biosystems Dynamics Research, Kobe 650-0047, Japan*
[2] *Nonequilibrium Physics of Living Matter RIKEN Hakubi Research Team, RIKEN Center for Biosystems Dynamics Research, 2-2-3 Minatojima-minamimachi, Chuo-ku, Kobe 650-0047, Japan*
[3] *Department of Physics, Emory University, Atlanta, GA, USA*
[4] *Department of Physics, Syracuse University, Syracuse, New York 13244, USA*
[5] *BioInspired Institute, Syracuse University, Syracuse, New York 13244, USA*

* takaki.yamamoto@riken.jp
† memanning@gmail.com

I. TIME SCALES FOR EDGE SHRINKING AND GROWING

As discussed in the main text, we expect that a cell center of mass diffuses on the timescale associated with either edges shrinking to zero and inducing a T1 transition or growing beyond unity and triggering a T1 transition in a nearby edge. While in the main text we focus on the diffusion timescale of an edge in the absence of any boundary conditions, here we numerically study a toy first-passage-time problem in order to determine if the first-passage time statistics with absorbing boundary conditions are different from the simple diffusion problem.

Specifically, we are interested in the behavior of an edge subject to the dynamics given by Eq. (4) and Eq. (3) in the main text, and in calculating the time it takes for such an edge to either shrink to zero length (where the full model would attempt a T1 transition) or grows significantly longer than unity (where it is likely that nearby edges exhibit a T1) in the absence of other interactions.

To quantify this upper edge length cutoff, we analyze the edge-length distributions in the full numerical simulations, and Fig. S1 shows the maximum value of edge length in our finite simulation box, $l_{\max}$, as a function of model parameters. Since Fig. S1 suggests that a T1 transition is induced to change the geometry when the edge length exceeds $\sim 1.2 \sim 2l_{\rm hex}$ ($l_{\rm hex} = \sqrt{2\sqrt{3}}/3 \approx 0.62$), we use that value $l_l = 2l_{\rm hex}$ as the upper length cutoff in our toy model.

We numerically solve Eq. (4) using Eq. (3) with $l_{ij} = l$ and $\Delta\lambda_{ij} = \Delta\lambda$ with the initial edge length $l = l_{\rm hex}$ and then calculate the time $\tau_{\rm FPT}$ when the edge length satisfies $l < 0$ or $l_l < l$ for the first time, which is a first passage time problem. We used forward Euler method with a time step $\delta t = 0.01$. $\Delta\lambda$ is sampled at the initial time point $t = 0$ from the normal distribution $N(0, \sigma^2)$, which is the stationary distribution of Eq. (3).

Figure S2(a) shows the average first passage time $\langle\tau_{\rm FPT}\rangle$ calculated from 100 trajectories for each set of parameters (σ, τ). For each simulation, we stopped calculation if the edge length keeps the condition $0 < l < l_l$ within 10^5 natural time units. We avoid such trajectories as rare events in calculating $\langle\tau_{\rm FPT}\rangle$; they were only observed for $(\sigma, \tau) = (0.02, 0.01)$, where 9 of 100 trajectories did not satisfy $l < 0$ or $l_l < l$ within 10^5 natural time units. To investigate the scaling behavior in the small- and large-τ regimes, we also plot $\langle\tau_{\rm FPT}\rangle\sigma^2$ vs. τ and $\langle\tau_{\rm FPT}\rangle\sigma$ vs. τ in Fig. S2(b) and (c). Figure S2(b) and (c) suggest that $\langle\tau_{\rm FPT}\rangle \sim 1/\sigma^2\tau$ and $\langle\tau_{\rm FPT}\rangle \sim 1/\sigma$ in the small- and large-τ regimes, respectively.

As discussed in the main text, an analytical calculation of the diffusion of a single edge in the absence of any other interactions gives $\mathrm{MSD}_l(t) = 2\sigma^2\tau t + 2\sigma^2\tau^2(\exp(-t/\tau) - 1)$, in which $\mathrm{MSD}_l(t) \sim 2\sigma^2\tau t$ ($t \gg \tau$) and $\mathrm{MSD}_l(t) \sim \sigma^2 t^2$ ($\tau \gg t$) [1].

Therefore, in the small-τ regime, our numerical result for the first passage time, $\langle\tau_{\rm FPT}\rangle \approx l_{\rm hex}/2\sigma^2\tau$, exhibits the same scaling as the analytical MSD prediction. Interestingly, the MSD scaling for the large τ regime is also consistent with the large τ FPT result: $\langle\tau_{\rm FPT}\rangle \approx l_{\rm hex}/\sigma$.

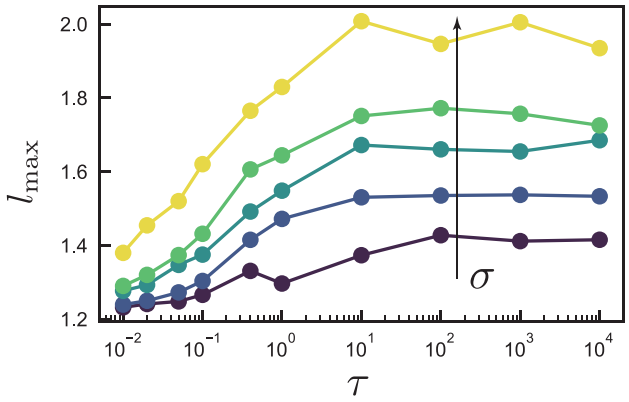

Fig. S1. **Maximum edge length $l_{\max}$.** $l_{\max}$ vs. τ for $\sigma \in [0.02, 0.05, 0.10, 0.15, 0.30]$ (from dark color to light color).

II. SCALING OF THE DIFFUSION CONSTANT FOR THE RESETTING AND RESAMPLING MODELS

We show the scaling of the diffusion constant D with respect to σ and τ in the small and large τ regime for the resetting and resampling models in Fig. S3. In both models, as in the persistent model, D asymptotically approaches

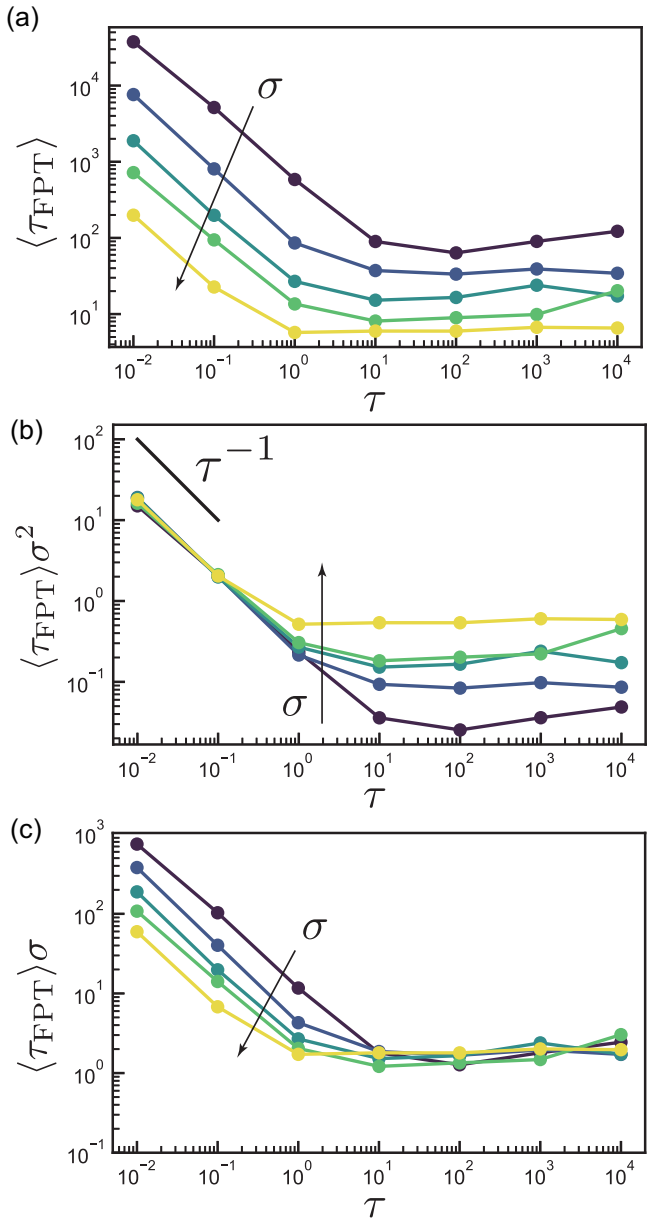

Fig. S2. **Scaling behavior of the average first passage time $\langle \tau_{\mathrm{FPT}} \rangle$ in the 2 vertex model.** (a) $\langle \tau_{\mathrm{FPT}} \rangle$ vs. τ. (b) $\langle \tau_{\mathrm{FPT}} \rangle \sigma^2$ vs. τ. The solid line is a guide for eyes indicating the power law τ^{-1}. (c) $\langle \tau_{\mathrm{FPT}} \rangle \sigma$ vs. τ. $\sigma \in [0.02, 0.05, 0.10, 0.15, 0.30]$ (from dark color to light color).

$D \sim \sigma^2 \tau$ in the small τ regime and $D \sim \sigma/\tau$ in the large τ regime. We note that in some resampling model simulations where τ and σ are near the extremes of model parameter values, numerical instabilities occur during the simulation and so we do not include those data points in the figures.

III. ANALYSIS OF TRAPPED EDGES

We note that in the persistent model, a large number of very short edges appear when τ is large (Fig. 2(a-d)), suggesting that some edges might be trapped close to zero length.

To test whether these have an impact on the dynamics at large τ we focus on higher-order vertices, which are vertices where more than three cells meet, *i.e.* rosette structures. A CVM study by Yan *et al.* in the limit of zero fluctuations recently showed that rosette structures can rigidify the epithelial tissue [2]. We want to study whether the

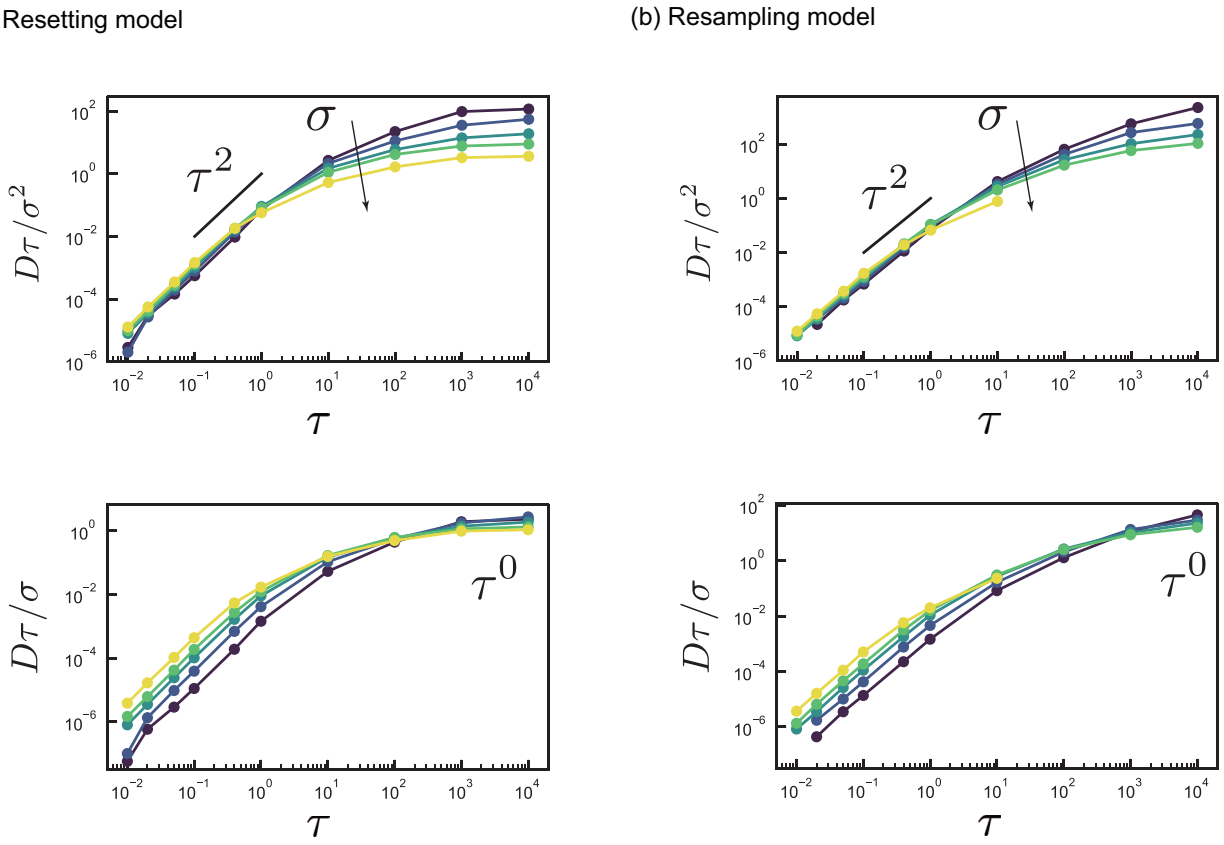

Fig. S3. **Scaling of D with respect to σ and τ in the small and large τ regime for the (a) resetting and (b) resampling models.** Data collapse in a plot of $D\tau/\sigma^2$ vs. τ demonstrates the scaling relation $D \propto \sigma^2\tau$ in the small τ regime. The solid line is a guide to the eye indicating the power law τ^2. $\sigma \in [0.02, 0.05, 0.10, 0.15, 0.30]$ (from dark color to light color). Data collapse in a plot of $D\tau/\sigma$ vs. τ demonstrates the scaling relation $D \propto \sigma/\tau$ in the large τ regime. $\sigma \in [0.02, 0.05, 0.10, 0.15, 0.30]$ (from dark color to light color).

rigidification of the tissue driven by rosette structures slows down the dynamics in our model in the large-τ regime.

However, unlike ref.2, by construction our model only contains 3-fold coordinated vertices. Nevertheless, we hypothesize that in a dynamic simulation with finite fluctuations, vertices connected by very short interfaces restrict the dynamics in a manner similar to multi-fold coordinated vertices. Although higher-fold vertices are generically unstable in the fluid phase in CVMs with spatially homogeneous parameters [3], some of us previously reported similar behavior in a 2D CVM with extra interfacial tensions between two cell types, where nearly-4-fold vertices (with very short edges) are stabilized at the heterotypic interface [4]. Therefore it is not surprising that fluctuating heterotypic tensions could drive similar phenomena.

This is also consistent with our previous qualitative analysis of cellular structures: Fig. 2 (b, c) shows that an increasing number of very short edges, highlighted by square symbols, is associated with rigidification in the large-τ regime.

To better understand how short edges affect the overall dynamics in this model, we study their individual dynamics. Specifically, we track edges, indexed by i, that reach the threshold $l_{\text{th}} = 0.03$ for checking a T1 transition. At every subsequent timestep where the edge length continuously remains below l_{th}, we record the edge length $l^i(t_T)$, where t_T is the time since the edge first crossed l_{th}.

To quantify this behavior, we study histograms of the edge lengths $f(l^i)$ for various values of this trapping time t_T (Fig. S4). For all but the longest timescales, there is a peak around $l \sim 0.005$, which is much smaller than the imposed T1 threshold l_{th}, suggesting there is a population of edges where the dynamics drives them to remain very short. Such edges must remain short either because accepting a T1 transition increases the energy, and so T1 steps are rejected, or because they alternate between T1 events at every timestep. In either case, the geometry and the tensions are such that it is energetically favorable for the edge to remain very short over multiple timesteps, resulting in a "trapped" short edge that functions very much like a multi-fold coordinated vertex.

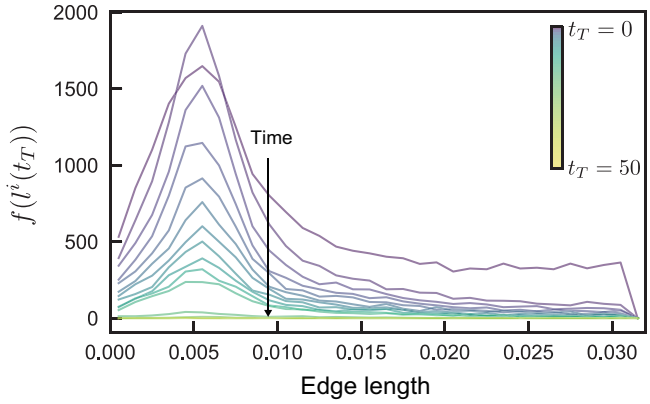

Fig. S4. **The time-evolution of the distribution $f(l^i(t_T))$ of the length $l^i(t_T)$ of the edges experiencing T1 events.** The data for $\tau = 10$ and $\sigma = 0.15$ is shown as an example. The color of the curves logarithmically maps the time t_T ranging between 0 and 50 natural time unit.

Figure S5(a) shows an integral of these length histogram over all time windows, $F(l^i) = \sum_{t_T} f(l^i(t_T))$, which similarly exhibits a prominent peak $l \sim 0.05$, highlighting a characteristic length for edges that are trapped. We randomly sampled 100 edges and 200 T1 events for each edge to plot Fig. S5(a). To formally define "trapped edges", we use this peak to define a new threshold lengthscale l^* shown by the vertical line in Fig. S5(a), that provides an upper bound to the length of the vast majority of trapped edges, see discussion in section III A. This allows us to formally define all edges with length $l < l^*$ as trapped edges that may be functioning as "effective high-order vertices". We can also define a "trapped edge lifetime" τ_T corresponding to the number of natural time units where the edge continuously maintains a length less than l^*.

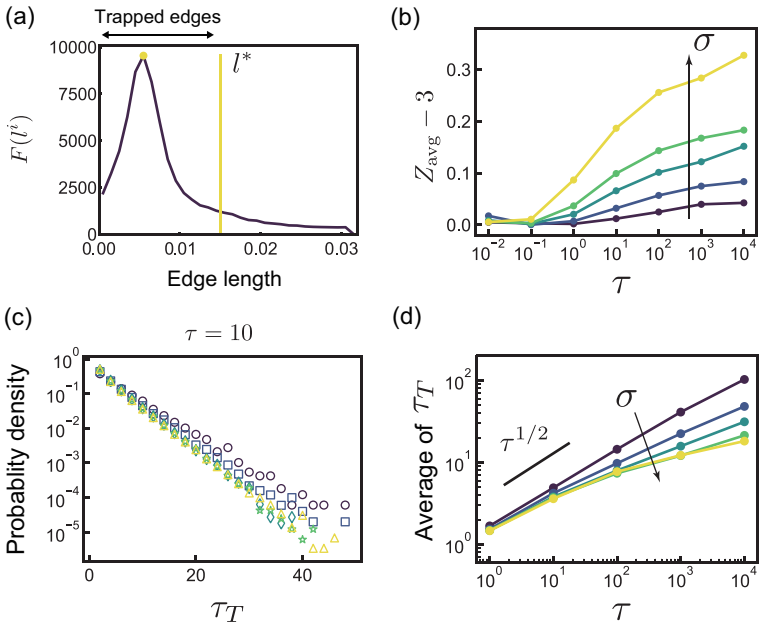

Fig. S5. **Properties of trapped edges.** (a) Time-integrated distribution of edge lengths, $F(l^i)$, defined in the main text. Trapped edges are defined as the population of edges in the peak, thresholded by the edge length by l^* as indicated by the yellow vertical line. (b) The average vertex coordination number per frame $Z_{\rm avg}$ subtracted by 3 is plotted against τ. In (b), we set $l^* = l_{\rm th}$ for some data points $(\tau, \sigma) = (0.01, 0.1/0.15/0.3), (0.1, 0.02)$, since the distributions $F(l^i)$ were too broad to determine the threshold l^* for the trapped edges for these parameter values. (c) Semi-log plots of the probability distribution of the life time τ_T of the trapped edges for $\tau = 10$. (d) The average lifetime τ_T of the trapped edges is plotted against τ. The solid line is a guide for eyes indicating the power law $\tau^{1/2}$. In (b-d), $\sigma \in [0.02, 0.05, 0.10, 0.15, 0.30]$ (from dark color to light color).

To quantify the density of these effective higher-order vertices, we calculate $Z_{\rm avg}$, which is the average vertex coordination number $Z = 2E/V$, where E and V are the number of edges and vertices per timestep [2] : if we have no trapped edges and only 3-fold vertices, $Z = 3$. We calculate $Z_{\rm avg}$ as $Z_{\rm avg} = 2(E_0 - T_{\rm avg})/(V_0 - T_{\rm avg})$, where $T_{\rm avg}$ is the average number of trapped edges per timestep. In Fig. S5(b), we plot $Z_{\rm avg} - 3$ with respect to τ for different σ. We find that $Z_{\rm avg} - 3$ increases monotonically as τ and σ increase.

Moreover, since our system is dynamic (unlike the system in ref.2), the persistence time of multi-fold coordinated vertices may be important. Therefore, we also investigate the lifetime of trapped edges τ_T, with normalized histograms shown in Fig. S5(c) and Fig. S6. The distribution is consistent with an exponential in the moderate τ regime ($\tau \sim 10$) as shown in Fig. S5(c), while it looks nearly power-law, with a large-scale cutoff, in the large-τ regime ($\tau \sim 1000$, see Fig. S6). Although the mechanisms driving these distributions remains unclear, we can nevertheless extract the average lifetime of trapped edges $\langle \tau_T \rangle$ as a function of model parameters, shown in Fig. S5(d). The average lifetime of trapped edges increases dramatically with increasing τ, and also increases slightly with decreasing σ. Taken together, these results suggest that there is a systematic increase in the fraction and persistence of effectively multi-fold coordinated vertices at large τ, which, in the absence of other effects, should tend to rigidify the system.

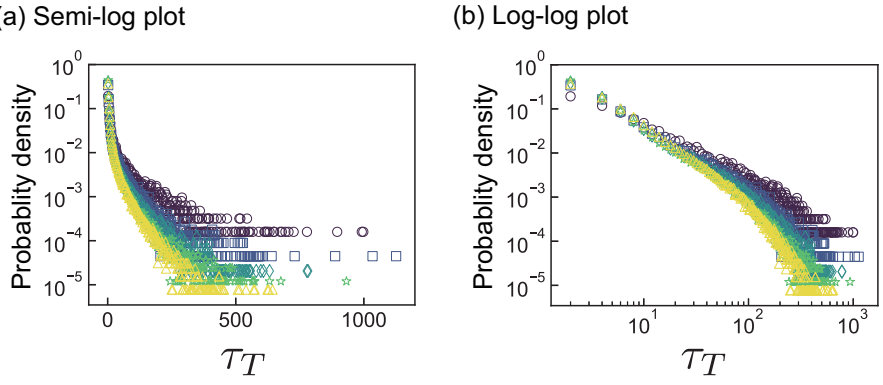

Fig. S6. **The probability distribution of the life time τ_T of the trapped edges.** (a) Semi-log and (b) log-log plots of the probability distribution τ_T for $\tau = 1000$. $\sigma \in [0.02, 0.05, 0.10, 0.15, 0.30]$ increase from dark color to light color (circle: $\sigma = 0.02$, square: $\sigma = 0.05$, diamond: $\sigma = 0.10$, star: $\sigma = 0.15$, triangle: $\sigma = 0.30$).

One obvious question, especially given the important role of effective multi-fold coordinated vertices, is whether our results depend strongly on our choice of how to resample the stress in the newly created edges after a T1 swap. The "persistent" model we have considered so far gives the new edge after a T1 swap the same tension as the old edge, which will clearly favor trapped edges where the tension is larger and contractile. Therefore, we also investigate more democratic ways of sampling tensions in the new T1 edge, illustrated schematically in Fig. 1 (b) and (c), which we term "resetting" and "resampling" models.

Figure 6 shows that, as expected, resetting and resampling models generate the same diffusion constants as the persistent models in the small-τ regimes, consistent with the hypothesis that fluctuation-driven diffusion, which should be the same in all models, dominates at low τ. In addition, there is still non-monotonic behavior in all three models, with the diffusion constant decreasing at large τ, while there is an obvious increase in the diffusion constant at larger τ in the resetting and resampling models compared to the persistent model.

In order to see if multi-fold coordinated vertices play an important role in rigidification in the large τ regime of the resetting and resampling models, we measured the fraction of trapped edges and the trapping time for both models. In general, we follow the same procedure outlined above for the persistent model. We note that in some resampling model simulations where τ and σ are near the extremes of model parameter values, numerical instabilities occur during the simulation and so we do not include those data points in the figures. As shown in Figs. S7 and S8, especially in the resampling model, there was not a significant increase in the number of trapped edges, and again only a modest increase in the trapping time. Given that the resampling model also exhibits a nonmonotonic curve for the diffusion constant with increasing τ, this suggests that, at least in the resampling case, the trapped edges are not responsible for the decrease in diffusion observed at large τ. We conclude that rigidification driven by multi-fold coordinated vertices is a potential mechanism contributing to reduced diffusion in some models, but clearly not sufficient to explain the non-monotonoicity in all the models we studied. An interesting question for future work remains whether and how short trapped edges are contributing to the rigidification in the persistent model, where they are common.

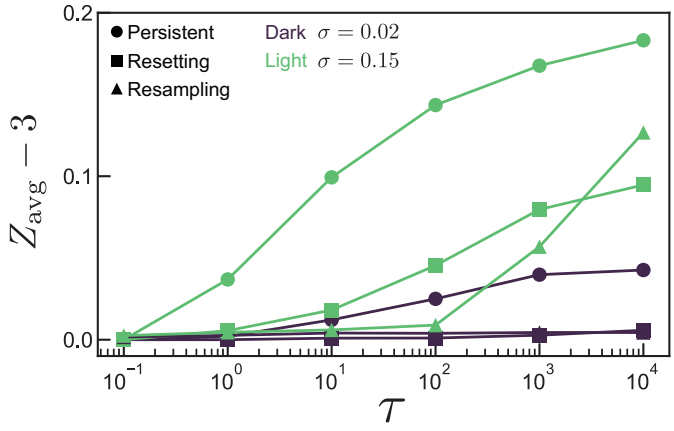

Fig. S7. **Comparison $Z_{\rm avg} - 3$ between three models**: the persistent model (circle), the resetting model (square), the resampling model (triangle). $Z_{\rm avg} - 3$ vs. τ for the three models, respectively. Dark and light markers represent the data with $\sigma = 0.02$ and $\sigma = 0.15$, respectively. The distributions $F(l^i)$ were too broad to determine the threshold l^* for the trapping edges in the following data points: $(\tau, \sigma) = (0.1, 0.02)$ in the persistent model, $(\tau, \sigma) = (0.1, 0.02/0.15), (1, 0.02)$ in the resetting model, $(\tau, \sigma) = (0.1, 0.02/0.15)$, $(1, 0.02/0.15)$, $(10, 0.02/0.15)$, $(100, 0.02)$, $(1000, 0.02)$, $(10000, 0.02)$ in the resampling model. We hence set $l^* = l_{\rm th}$ for these data points.

A. Definition of the threshold l^* of the trapped edges

We first detected a maximum peak at $l = l_{\rm max}$ in the time-integrated distribution $F(l^i)$ as indicated by a yellow circle marker in Fig. S5(a). We next subtracted the minimum frequency in the range $l_{\rm max} \leq l \leq l_{\rm th}$, as the background, from the time-integrated distribution. Using this background-subtracted distribution, we finally determined the threshold l^* as the minimum edge length at which the frequency is below 10% of the maximum frequency at $l = l_{\rm max}$. In Fig. S4, we show an example of histograms of the edge lengths $f(l^i)$ for various values of the trapping time t_T.

[1] A. S. Bodrova, A. V. Chechkin, A. G. Cherstvy, H. Safdari, I. M. Sokolov, and R. Metzler, Scientific Reports **6**, 30520 (2016).
[2] L. Yan and D. Bi, Physical Review X **9**, 011029 (2019).
[3] M. A. Spencer, Z. Jabeen, and D. K. Lubensky, The European Physical Journal E **40**, 2 (2017).
[4] D. M. Sussman, J. M. Schwarz, M. C. Marchetti, and M. L. Manning, Physical Review Letters **120**, 058001 (2018).

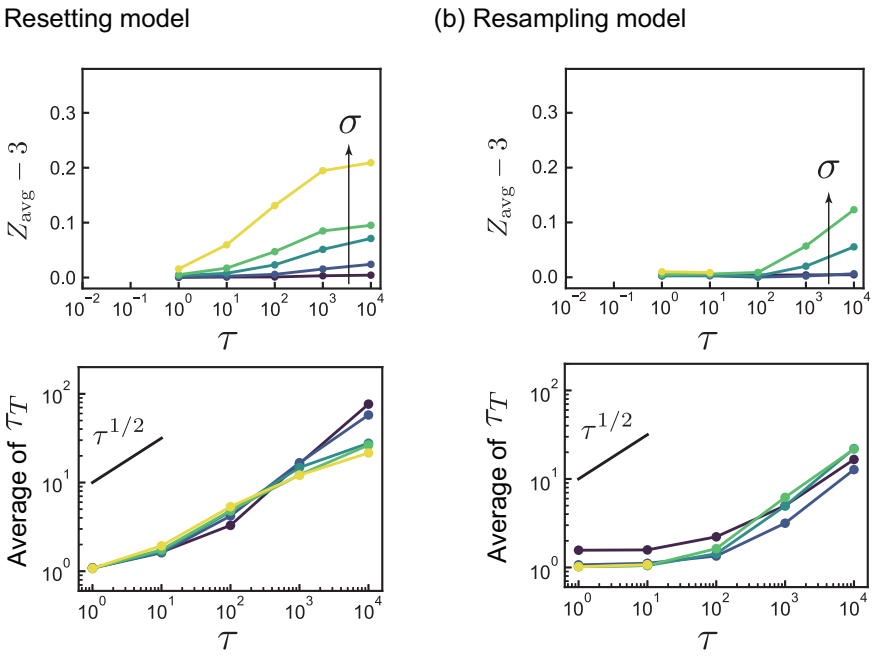

Fig. S8. **Properties of trapped edges for the resetting and resampling models.** In the top panels of (a) resetting model and (b) resampling model, the average vertex coordination number per frame $Z_{\rm avg}$ subtracted by 3 is plotted against τ. In the bottom panels, the average lifetime τ_T of the trapped edges is plotted against τ. The distributions $F(l^i)$ were too broad to determine the threshold l^* for the trapping edges in the following data points: $(\tau,\sigma)=(1,0.02)$ in the resetting model and $(\tau,\sigma)=(1,0.02/0.05/0.1/0.15/0.3),(10,0.02/0.05/0.1/0.15),(100,0.02),(1000,0.02),(10000,0.02)$ in the resampling model. The solid line is a guide for eyes indicating the power law $\tau^{1/2}$. In (a) and (b), $\sigma\in[0.02,0.05,0.10,0.15,0.30]$ (from dark color to light color).